lubricants

MDPI

Article

Effect of Temperature and Surface Roughness on the Tribological Behavior of Electric Motor Greases for Hybrid Bearing Materials

Daniel Sanchez Garrido, Samuel Leventini and Ashlie Martini *

Department of Mechanical Engineering, University of California Merced, 5200 N. Lake Rd., Merced, CA 95343, USA; dsanchezgarrido@ucmerced.edu (D.S.G.); sleventini@ucmerced.edu (S.L.)
* Correspondence: amartini@ucmerced.edu

Abstract: Greased bearings in electric motors (EMs) are subject to a wide range of operational requirements and corresponding micro-environments. Consequently, greases must function effectively in these conditions. Here, the tribological performance of four market-available EM greases was characterized by measuring friction and wear of silicon nitride sliding on hardened 52100 steel. The EM greases evaluated had similar viscosity grades but different combinations of polyurea or lithium thickener with mineral or synthetic base oil. Measurements were performed at a range of temperature and surface roughness conditions to capture behavior in multiple lubrication regimes. Results enabled direct comparison of market-available products across different application-relevant metrics, and the analysis methods developed can be used as a baseline for future studies of EM grease performance.

Keywords: grease; hybrid bearings; electric vehicles; electric motors; friction and wear

Citation: Sanchez Garrido, D.; Leventini, S.; Martini, A. Effect of Temperature and Surface Roughness on the Tribological Behavior of Electric Motor Greases for Hybrid Bearing Materials. *Lubricants* **2021**, *9*, 59. https://doi.org/10.3390/lubricants9060059

Received: 5 April 2021
Accepted: 5 May 2021
Published: 24 May 2021

1. Introduction

Electric vehicles (EVs) are emerging as the future of transportation as the market shifts from internal combustion engine vehicles (ICEVs) to electrification [1,2]. Although EVs are more energy efficient than ICEVs, energy losses in electric motors (EMs) are still considerable [3,4]. Mechanical losses in EMs mainly derive from friction in bearings [3,5,6]. Further, about 40–60% of early EM failures are said to be premature bearing faults [4,7], with most failures being due to improper lubrication [7]. Grease is used in 80–90% of rolling bearings [3,8], and, consequently, failed grease lubrication is the predominant cause of EM bearing failure [9–11]. Another source of premature bearing failure that adversely affects EM life is exposure to electrical environments, like those found in EVs [4]. Formulating greases for EV applications is a particular challenge because of key differences between the environment and operating conditions in EVs and those experienced by greases in traditional ICEVs, particularly, speed, temperature, and materials. These conditions are also experienced by greases in industrial EMs.

First, EMs in industrial applications and EVs are operated at high speeds. Grease lubrication is very dependent on speed and can exhibit inverse Stribeck behavior where friction is low at low speeds [12,13]. This deviation from the behavior of lubricating oils is most significant at low λ ratios, i.e., small film thickness to effective surface roughness ratios [12]. In addition, at low speeds or nominal boundary conditions, friction is determined by grease thickener alone and is lower than that predicted for base oil [12,14,15]. Grease film thickness is larger than calculated for a base oil at low speeds, and the same or smaller than calculated at higher speeds [5,16–21]. Therefore, the wide range of speeds expected for EMs introduces additional challenges when selecting or designing greases for EV or industrial applications.

High temperature is another challenge for grease lubrication in EMs. Although some increase in temperature can be beneficial because it helps grease bleed and, thus, resupplies

lubricant to the bearing contact track [16,22], high temperatures can also generate harsh operating environments. High rotor speeds generate heat [3], and EMs can reach operating temperatures of 150 °C [23] or even 180 °C [24] for some applications. Therefore, greases used in EM bearings can experience thermal degradation in the form of oxidation and decreased lubricating capabilities as a result of EM operating environments [9–11]. More specifically, grease can suffer thermo-oxidation degradation as a result of high temperature during bearing operation [9], and, at temperatures >120 °C, oxidation ages grease which affects its lubricity and decreases grease life [8,25]. Note that aging will affect the rheological properties of the grease differently depending on its formulation [14]. The result of high temperature and high speed is grease degradation, which affects the chemical composition of the grease, as well as its physical properties that can adversely affect film formation, leading to ineffective lubrication [9].

Another challenge for grease lubrication of EMs is that the materials of bearings may differ from those in traditional motors. Specifically, many EM bearings have ceramic components that act as insulators to mitigate issues related to stray current. Stray current can damage both the bearing and the grease, as well as generate heat, which can cause localized melting of metal surfaces, cause pitting, break particles loose, and embrittle materials [26,27]. In addition, grease that is electrically conductive can amplify these effects and accelerate bearing damage [27]. Current discharge also causes grease degradation by thermal-oxidation and evaporation of the base oil and additives, which then makes grease rigid [26]. The adverse effects of stray current on bearing failure will be more prevalent as EVs become a larger portion of the transportation sector [4]. Therefore, it is necessary to better understand how the electric environment influences EM bearing/grease systems [4] and develop tribological knowledge of non-traditional bearing materials operating in EM environments.

The most common ceramic material used for such applications is silicon nitride. Silicon nitride is suitable for bearings due to its mechanical properties across wide temperature ranges, electrical insulation, thermal shock resistance, excellent fracture toughness, wear resistance, long life, and reliable low maintenance operation [28,29]. Silicon nitride serves as a bearing insulator [26] that disrupts stray current in EMs and, thus, minimizes grease thermal degradation and melting of material that leads to wear. Often, silicon nitride is used in hybrid bearings that consist of ceramic rolling elements and traditional steel raceways [26]. Hybrid bearings have been found to last longer than predicted based on the Lundberg-Palmgren theory [30], and grease life with hybrid bearings was found to be up to four times longer than with traditional all steel bearings [26]. However, there are issues associated with the use of ceramic bearing elements, particularly related to lubricant additives. For example, phosphorus-based additives were found to not react with silicon nitride as they would with steel so the tribofilms formed were not effective in improving silicon nitride bearing life [31–33]. Another potential issue is that hybrid bearings experience higher contact stress than all steel bearings under the same applied load [30], due to the higher hardness of ceramics, which corresponds to smaller contact areas.

The aforementioned challenges with grease lubrication in EMs can be partially addressed through design or selection of greases specifically for EM environments. Thickener type, base oil type, and viscosity all have a significant impact on film thickness and friction for grease lubricated rolling/sliding contacts [12–14,34]. Greases are continually changing, as formulators and designers seek to optimize lubrication in different operating environments, while remaining compatible with component materials. For example, recent studies have used nanotechnology to create novel additives for grease formulations that improve lubricity and grease life [3,35–37]. Another study focused on extending EM bearing life by reducing grease degradation and found this can be achieved with the use of an antioxidant and high-temperature composite grease formulation [9]. Continued research in the area of grease formulation is crucial because grease behavior is extremely application dependent [22].

Grease optimization often focuses on identifying the best combination of base oil and thickener for EM applications. Studies have evaluated the lubrication mechanisms associated with synthetic or mineral base oil with urea or lithium thickener. For instance, an ester-polyurea grease used for EMs with silicon nitride ceramic rolling elements was found to have excellent life, resist high operating temperatures, and withstand high speeds experienced in the motor [26]. Synthetic base oils resist higher temperatures, while generating low friction and improving service life [3,38]. Although lithium thickened greases are currently the most widely used [8], some studies suggest urea thickened grease may generate lower friction and thicker films, as well as have a closer correlation to typical Stribeck behavior than lithium thickened greases [12]. A study comparing custom polyurea and lithium thickened greases on bearing steel was performed to characterize performance at 25, 70, and 120 °C and average surface roughness of 10, 100, and 200 nm [12]. Polyurea greases were shown to have the lowest friction at low speed, average surface roughness of 100 nm Ra, and temperatures of 70 and 120 °C. Further, it was reported that polyurea had thicker low-speed films than lithium greases [12].

Based on the current findings, it is evident that both base oil and thickener affect grease performance and that optimizing this performance for EM applications requires characterization at the conditions in which the motor will operate. Specifically, EM greases are subject to higher temperatures and may be required to function with different bearing materials than traditional applications. Here, we tested the tribological performance of four commercially available greases with formulations/additives designed for EM applications, with different combinations of mineral or synthetic base oil with lithium (complex) or urea thickeners. The study focused on lubrication of silicon nitride sliding on steel across a range of temperature and surface roughness conditions. The tribological performance of these greases and bearing materials was quantified in terms of friction and wear. Characterization included both ball-on-disk and 4-ball tests, as well as an analysis of the results in terms of lubrication regimes. Finally, the four greases were evaluated based on a ranking system that emphasized priorities for EM applications.

2. Materials and Methods

Four commercially available greases were studied, all of which were designed for EM applications, per manufacture specifications. All EM greases had an International Standard Organization Viscosity Grade (ISO VG) of 100 and a National Lubricating Grease Institute (NLGI) grade of 2, but with different combinations of thickener and base oil types. The specific greases studied were: synthetic-polyurea (SP), mineral-polyurea (MP), mineral-lithium (ML), and synthetic-lithium complex (SL). Note that, since the tested greases were commercially available, formulation details, such as additive composition and concentration, were not known. Table 1 provides the reported information for each grease.

Table 1. EM grease specifications.

EM Grease	Acronym	Base Oil Viscosity at 40 °C (cSt)	Base Oil Viscosity at 100 °C (cSt)	Base Oil Density at 15 °C (g/cm^3)	Dropping Point (ASTM D2265 °C)
Synthetic-polyurea	SP	100	14	0.85	250
Mineral-polyurea	MP	100	12	0.88	260
Mineral-lithium	ML	100	11	0.93	180
Synthetic-lithium complex	SL	100	14	0.85	260

Two types of experiments were conducted to characterize the tribological performance of the EM greases. First, a Rtec Instruments Multi-Function Tribometer equipped with a temperature chamber was used to perform unidirectional sliding ball-on-disk tests, illustrated in Figure 1a. In those tests, a silicon nitride ceramic bearing ball with a 9.525 mm diameter and an average surface roughness (Ra) of 20 nm were used. The ceramic balls

met grade 5 quality specifications. The flat disk had a 50.8 mm diameter and was made of hardened 52100 steel. An Allied High Tech Metprep 3 polisher was used to polish the disks with the use of a silicon carbide abrasive pad in water suspension for non-directional surface finish. The disks were polished to achieve a final average surface roughness of 10, 35, 60, 120, or 200 nm. Based on the ball and disk roughness, average composite roughness cases evaluated were 22, 40, 63, 122, and 201 nm. The surface roughness of the disks was measured using a Bruker DektakXT contact mode profilometer. Prior to testing, all testing surfaces were ultrasonically cleaned in heptane.

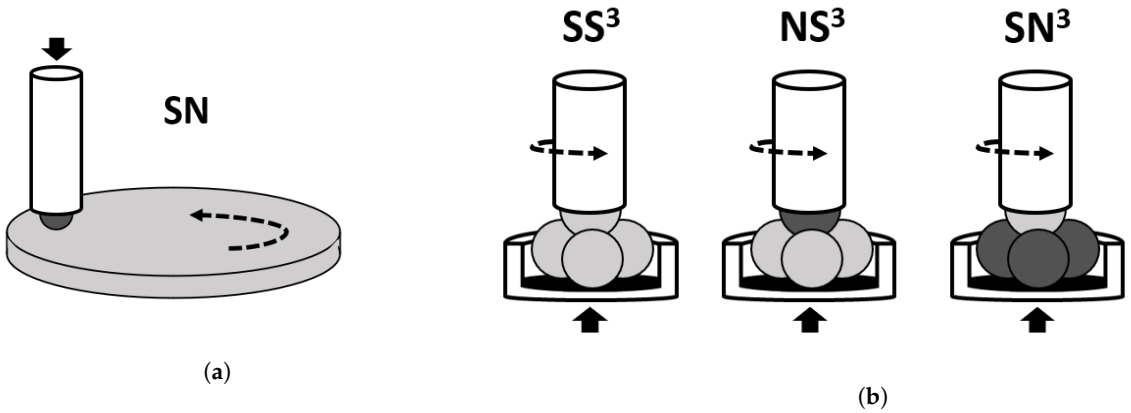

Figure 1. Greases were characterized using two test configurations: (**a**) Ball-on-disk and (**b**) 4-ball. The tests were performed with various combinations of steel (S) and silicon nitride ceramic (N) samples.

Ball-on-disk test parameters closely adhered to ASTM D5707-16 with some modifications to capture key conditions expected in EM environments, specifically, bearing material, temperature and surface roughness. The load was 10 N, corresponding to a maximum Hertz contact pressure of 1.2 GPa, and the sliding speed was 250 mm/s. Temperatures tested were 40, 100, and 150 °C. For each test, about 500 mm^3 (pea size amount) of grease was applied to lubricate the samples. A grease scoop was employed for tests at 40 °C to avoid starvation by continuously pushing the grease back onto the track [12,13,17,18]. All tests were run to 400 m total sliding distance, and each test condition was repeated three times.

Second, a Falex Multi-Specimen Test Machine was used to perform 4-ball testing, illustrated in Figure 1b. The 4-ball tests enabled different combinations of silicon nitride and hardened 52100 steel to be evaluated. Three different material configurations were tested:

- one steel rotating element on three steel stationary elements (SS^3),
- one silicon nitride ceramic rotating element on three steel stationary elements (NS^3), and
- one steel rotating element on three silicon nitride ceramic stationary elements (SN^3).

The SS^3 case resembled a traditional all steel bearing assembly, and the NS^3 case resembled a hybrid bearing assembly. The SN^3 resembled an inverted hybrid bearing assembly, meaning that the material typically used for the races was used as the rolling element and vice versa. All-ceramic bearings are infrequently used for standard applications, so the NN^3 configuration was not tested here. Test parameters followed the ASTM-D2266 standard. The load was 392 ± 2 N, which corresponds to a maximum Hertz contact pressure of 4.6 GPa for the SS^3 configuration and 5.2 GPa for the NS^3/SN^3 configurations. The silicon nitride ceramic test balls met grade 5 quality specifications and had a surface roughness of 20 nm Ra. The steel balls met grade 10 specifications and had 25 nm Ra. The speed was 1200 ± 60 revolutions per minute for 60 minutes, and the temperature was held at 75 °C ± 2 °C. All four greases were tested using each material configuration; the SS^3 and NS^3 results are averages of three tests, and the SN^3 results are averages of two tests.

Error was calculated as the difference between the maximum and minimum wear for each configuration and grease.

Images captured of the worn ball surfaces were obtained using a Leica Optical Microscope (Model DM 2500M) for both test methods. For the ball-on-disk tests, wear volume was calculated per ASTM G-133-05. Specific wear rate was then calculated by dividing the volume by the load and total sliding distance. For the 4-ball test, wear scar diameters were measured per ASTM D2266-01. Those measurements were then used to calculate the wear area of the scar.

3. Results

3.1. Ball-on-Disk Wear

Wear rate as a function of surface roughness for all EM greases is shown in Figure 2a. For smooth surfaces, the wear rates of the four greases are similar, although the lowest wear is observed for the MP. In contrast, there is more differentiation between the greases on rougher surfaces, where the ML consistently exhibits the lowest wear rate. In addition, for these testing parameters, greases with mineral base oil have lower wear rate than the synthetic base greases.

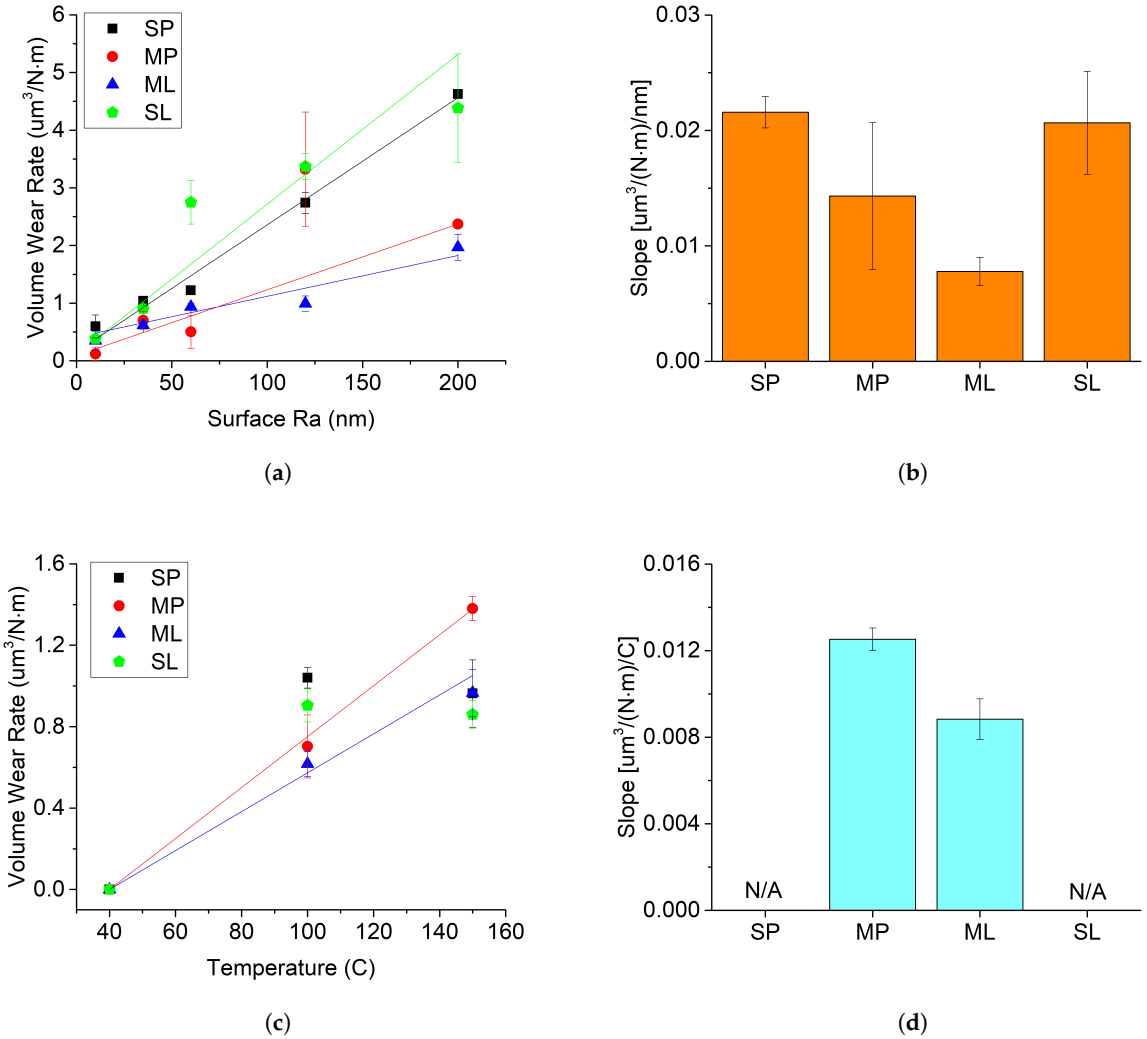

Figure 2. Wear results from EM grease ball-on-disk tests. (**a**) Wear rate as a function of roughness and (**b**) change in wear rate with roughness at 100 °C. (**c**) Wear rate as a function of temperature and (**d**) the change in wear rate with temperature at 35 nm Ra (composite Ra of 40 nm) for MP and ML.

The sensitivity of wear rate to changes in roughness was quantified as the slope of a linear fit to the data. Although this analysis is based on an assumption that wear rate increases linearly with roughness, the approach enables direct comparison of the greases. The slope calculated from a linear fit to the wear rate versus roughness data is shown in Figure 2b. This analysis indicates that wear rate with the ML grease is the least dependent on surface roughness. In addition, of the tested greases, greases with mineral base oil have less wear-roughness dependence than the synthetic base greases.

Wear rates at different temperatures are shown in Figure 2c. At 40 °C, there is no observable wear for any of the greases. The lowest wear rate at 100 °C is observed for the ML grease and, at 150 °C, is found for the SL grease. Additionally, at 100 and 150 °C, for the greases tested here, lithium thickened greases have a lower wear rate than their polyurea counterparts.

The temperature dependence of the wear rate is very different for synthetic versus mineral based greases. Specifically, the wear rate increases approximately linearly between 100 and 150 °C for the mineral greases, but is nearly constant for the synthetics. Due to this behavior, the linear approximation cannot be used to quantify the change of wear rate with temperature for the synthetic greases. However, the linear fit was performed for the mineral greases as shown in Figure 2d. The wear rate is less dependent on temperature for the ML grease than the MP grease.

3.2. Ball-on-Disk Friction

Friction results for each grease are shown in Figure 3. On average, friction increased with surface roughness for all greases (see Figure 3a). In addition, on most surfaces, friction was lowest for the SL grease. On the rougher surfaces, the ML also exhibited low friction behavior. For these tests, the lithium based greases had lower friction than the polyurea greases, except on the smoothest surfaces where the friction coefficient was below 0.08 for all greases.

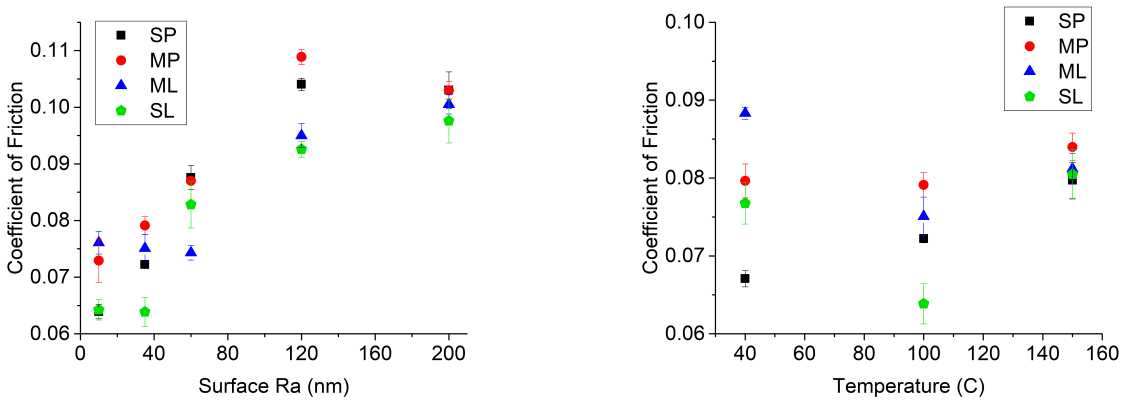

(**a**) (**b**)

Figure 3. Friction results from EM grease ball-on-disk tests. Friction coefficient (**a**) as a function of surface roughness at 100 °C and (**b**) as a function of temperature at 35 nm Ra (composite Ra of 40 nm).

Friction at three different temperatures is shown in Figure 3b. At 40 °C, the lowest friction was exhibited by the SP grease whereas, at 100 °C, the SL grease had the lowest friction. At both 40 and 100 °C, the friction was lower for synthetic greases than their mineral counterparts. At 150 °C, the friction coefficient was comparable for all four greases.

The friction trends with respect to roughness and temperature are not linear. This is primarily because both roughness and temperature affect the lubrication regime. Further, increasing temperature can promote grease bleed such that the degree of starvation decreases with increasing temperature [16]. So, the effect of these parameters on friction cannot be quantified using a simple linear fit. Instead, these trends will be analyzed in the context of the Stribeck curve, as discussed later.

3.3. 4-Ball Test

Results from the 4-ball tests are shown in Figure 4. ML had the lowest wear across all three bearing configurations. The performance of ML might be attributable to thicker lubricating films that provide more separation between interacting surfaces or better anti-wear film formation. For the SS^3 and NS^3 configurations, average wear increased as ML < MP < SP < SL. However, this trend cannot be directly explained since the 4-ball test is primarily measuring anti-wear behavior, and the additive composition of these commercial greases is unknown. For the SN^3 configuration, wear was high for all four greases, and large error bars precluded direct comparison between the greases.

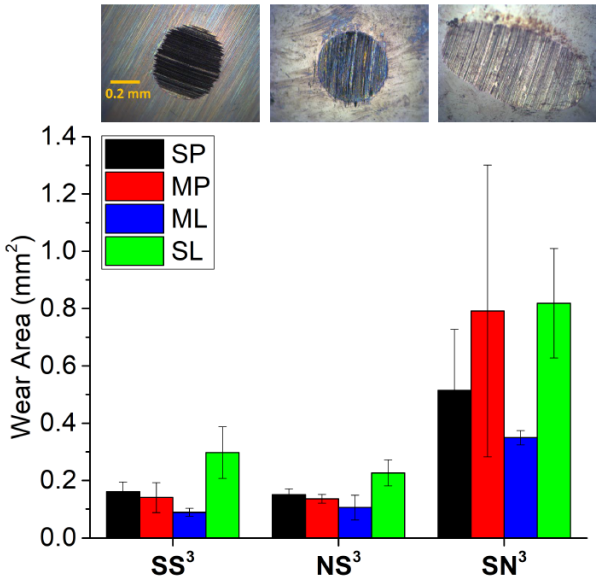

Figure 4. Wear area for four greases and three bearing configurations measured using the 4-ball test. Representative wear patterns (from left to right): SS^3 circular wear scar on steel ball, NS^3 circular wear scar on steel ball, and SN^3 elliptical wear scar on ceramic ball.

Comparing the different material combinations, for all greases, the lowest average wear was observed for NS^3, followed by SS^3 and then SN^3. The observation that wear for NS^3 was lower than that for SS^3 is consistent with previous reports that grease life with hybrid bearings is longer than with standard bearings [26]. Lower wear for NS^3 is also consistent with experimental and anecdotal observations that suggest longer lives for hybrid bearings than estimated by the Lundberg-Palmgren equations [30].

In contrast, the SN^3 configuration consistently had very high wear. This configuration also exhibited qualitatively very different behavior than the other two material pairs. As shown in the insets to Figure 4, the wear scars for the SS^3 and NS^3 configurations are circular, while those for the SN^3 are elliptical. The wear mechanism of the rotating elements determine and may cause non-circular wear scars of the stationary balls [39]. Therefore, the difference may be attributable to the hardness of the rotating element. For SN^3, the steel ball is the rotating element attached to the spindle (upper ball), while the three lower balls are silicon nitride. Material hardness affects material wear; a softer steel ball rotating on a harder ceramic ball causes the wear scar to elongate with increasing material deformation, thus causing relative displacement between the upper and lower balls.

4. Analysis & Discussion

4.1. Lubrication Regime Analysis

The friction results shown in Figure 3 suggests that changing either roughness or temperature caused a transition between lubrication regimes. The lubrication regime can be determined by the lambda ratio:

$$\lambda = \frac{h}{\left(Ra_{ball}^2 + Ra_{disk}^2\right)^{1/2}}, \tag{1}$$

where h is the film thickness, Ra_{ball} is the average roughness of the ball, and Ra_{disk} is the average roughness of the disk. Although the exact values of λ corresponding to transitions between lubrication regimes vary in the literature, they are often defined by $\lambda \gtrapprox 3$ for full film lubrication, $1 \lessapprox \lambda \lessapprox 3$ for mixed lubrication, and $\lambda \lessapprox 1$ for boundary lubrication [34,40,41]. However, these transition values are not absolute, and studies have shown that full film or mixed lubrication is possible even in cases where λ would typically suggest boundary lubrication (e.g., $\lambda \lessapprox 1$) [41].

For bearings, the λ ratio also affects contact fatigue life. Low λ ratios are associated with surface deformation and distress [2]. In the context of the conditions studied here, small surface roughness and low temperature conditions that correspond to higher λ ratios will have lower contact fatigue and longer life.

To calculate λ, we first had to determine film thickness. It is known that the film thickness of a grease may be larger or smaller than the film thickness for its base oil, depending on the operating conditions [12,34]. However, there is no standard equation or method of calculating grease film thickness that is applicable for all conditions. Therefore, as a first order approximation, we calculated film thickness using the Hamrock and Dowson equation [2] for central film thickness with parameters for the base oil:

$$h \approx h_c = 2.69R\left(\frac{U\eta}{ER}\right)^{0.67}(\alpha E)^{0.53}\left(\frac{W}{ER^2}\right)^{-0.067}(1 - 0.61e^{-0.73k}), \tag{2}$$

where U is the speed, R is effective radius, E is effective elastic modulus, α is the pressure-viscosity coefficient, η is the ambient viscosity, W is the load, and $k = 1$ for a spherical geometry. Most of these parameters are constant for the ball-on-disk tests. However, the ambient viscosity and pressure-viscosity coefficient were calculated for each test based on the rheological properties of the base oil and the temperature. Table 2 summarizes the film thickness and λ ratio for each EM grease, temperature, and roughness case considered in this study.

The friction measured from the ball-on-disk tests is plotted as a function of the calculated λ ratio to create a Stribeck curve in Figure 5. The large λ cases correspond to tests run on smooth surfaces and at lower temperatures. Conversely, rough surfaces and high temperatures lead to small λ ratios. The general shape of the Stribeck curve in Figure 5 indicates that our tests included the mixed regime, where friction decreases with λ, and the full film regime, where friction increases with λ.

Table 2. EM grease calculated film thickness (h_c in nm) and lambda (λ) ratio at all tested composite roughness and temperature combinations.

Temperature	°C	40	100	100	100	100	100	150
Composite Roughness	nm	40.3	22.4	40.3	63.3	121.7	201	40.3
SP	h_c	117	28.3	28.3	28.3	28.3	28.3	13.7
	λ	2.89	1.27	0.70	0.45	0.23	0.14	0.34
MP	h_c	151	27.8	27.8	27.8	27.8	27.8	11.3
	λ	3.74	1.25	0.69	0.44	0.23	0.14	0.28
ML	h_c	142	26.9	26.9	26.9	26.9	26.9	11.0
	λ	3.52	1.20	0.67	0.42	0.22	0.13	0.27
SL	h_c	117	28.3	28.3	28.3	28.3	28.3	13.7
	λ	2.89	1.27	0.70	0.45	0.23	0.14	0.34

The greases clearly exhibit full film at larger lambda ratios. In this regime, the lowest friction was exhibited by the SP and SL (synthetic greases). The mixed regime is clearly observed at small λ ratios. Here, as composite roughness increases, λ values decrease, and friction tends to increase. In mixed lubrication, the lowest friction was observed for the ML and SL (greases with lithium thickener). Across most of the lubrication regimes measured, SL had the best friction performance.

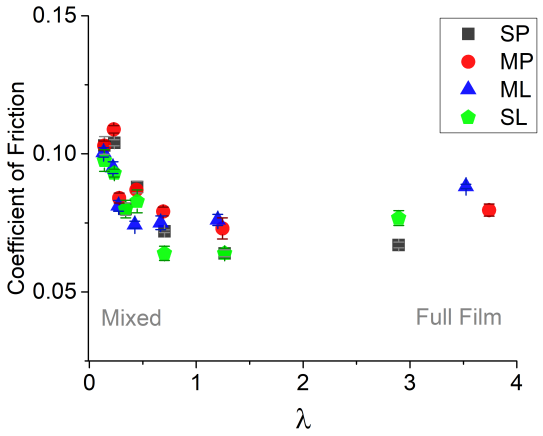

Figure 5. Stribeck curve based on measured friction and calculated λ ratios for four greases tested across all roughness and temperature conditions.

The transition between the full film and mixed lubrication regimes is important because both friction and wear are higher in the mixed regime due to asperity contacts in the interface. Therefore, it is desirable to remain in the full film regime as long as possible. To identify the λ ratio at which the full film-mixed transition occurs for each grease, we found the intersection of a linear fit to the data in the mixed regime and a linear fit to the data in the full film regime. The two largest λ ratios for each grease were fit for full film, and the three smallest λ ratios were fit for the mixed regime. Figure 6 shows the linear fits and their intersection which was identified as the transition lambda (λ_t). The λ_t values for each grease were found to be: SP at $\lambda_t = 0.48$, MP at $\lambda_t = 0.47$, ML at $\lambda_t = 0.37$, and SL at $\lambda_t = 0.58$.

The ML grease had the lowest λ_t, indicating that the interface would remain in the full film regime the longest with increasing temperature or roughness. However, it is important to note that ML also has higher friction in this transition region. So, ML's lower λ_t suggests the lubricant is able to maintain a thicker lubrication film than the other greases, but this comes at a cost of higher viscous friction. On the other hand, SL has a larger λ_t value but considerably lower friction than the rest of the tested greases in this transition range. In

fact, despite having a larger λ_t value, SL maintained lower friction at most test conditions. This analysis shows there is a compromise between low friction in full film lubrication and how long the interface will remain in that regime before the onset of mixed lubrication.

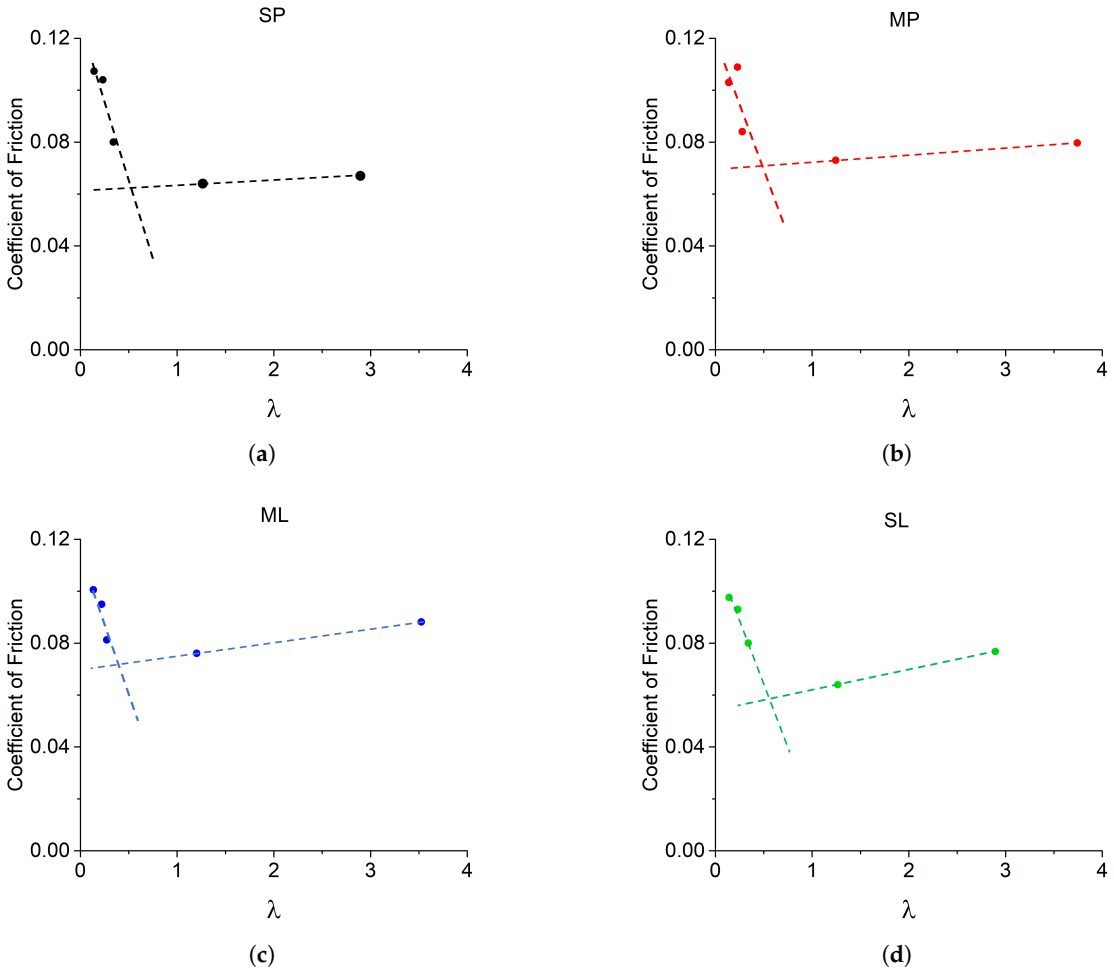

Figure 6. Independent linear fits performed for the mixed and full film regimes for (**a**) SP, (**b**) MP, (**c**) ML, (**d**) SL. The intersection of the two lines corresponds to the transition lambda λ_t.

4.2. Predicted Lubrication Regime Transitions

The λ ratio determines lubrication regime, as well as contact fatigue. In our study, this critical ratio is determined by surface roughness, grease properties and temperature. So, for a given grease, roughness, and temperature, the λ value can be calculated, and the conditions at which the lubrication regime transitions to mixed can be predicted.

Surface roughness affects this calculation directly, as it appears in the denominator of Equation (1). Temperature indirectly affects the film thickness as calculated using Equation (2) through its effect on η and α. The grease itself determines the values of η and α and their temperature dependence. To predict λ for any temperature T, we used a linear equation for $\alpha(T)$ and the Vogel equation [2] for $\eta(T)$, both fit to available grease data. Then, λ was calculated directly using the equations for $\alpha(T)$ and $\eta(T)$, combined with Equations (1) and (2).

This analysis was performed for each grease at temperatures ranging from 30 to 200 °C and composite roughness values from 20 to 200 nm Ra. The predicted λ values are shown as color contour plots in Figure 7. In addition, shown are horizontal planes corresponding to λ_t, the ratio at the transition between mixed and full film lubrication, identified from the friction data for each grease in Figure 6. The intersection between this plane and the surface predicted as described above indicates the temperature and surface roughness at which the interface will transition from full film to mixed lubrication. Such an approach

can be used as part of the design process to guide selection of a grease, surface roughness specifications, or prescribed limits on operating conditions.

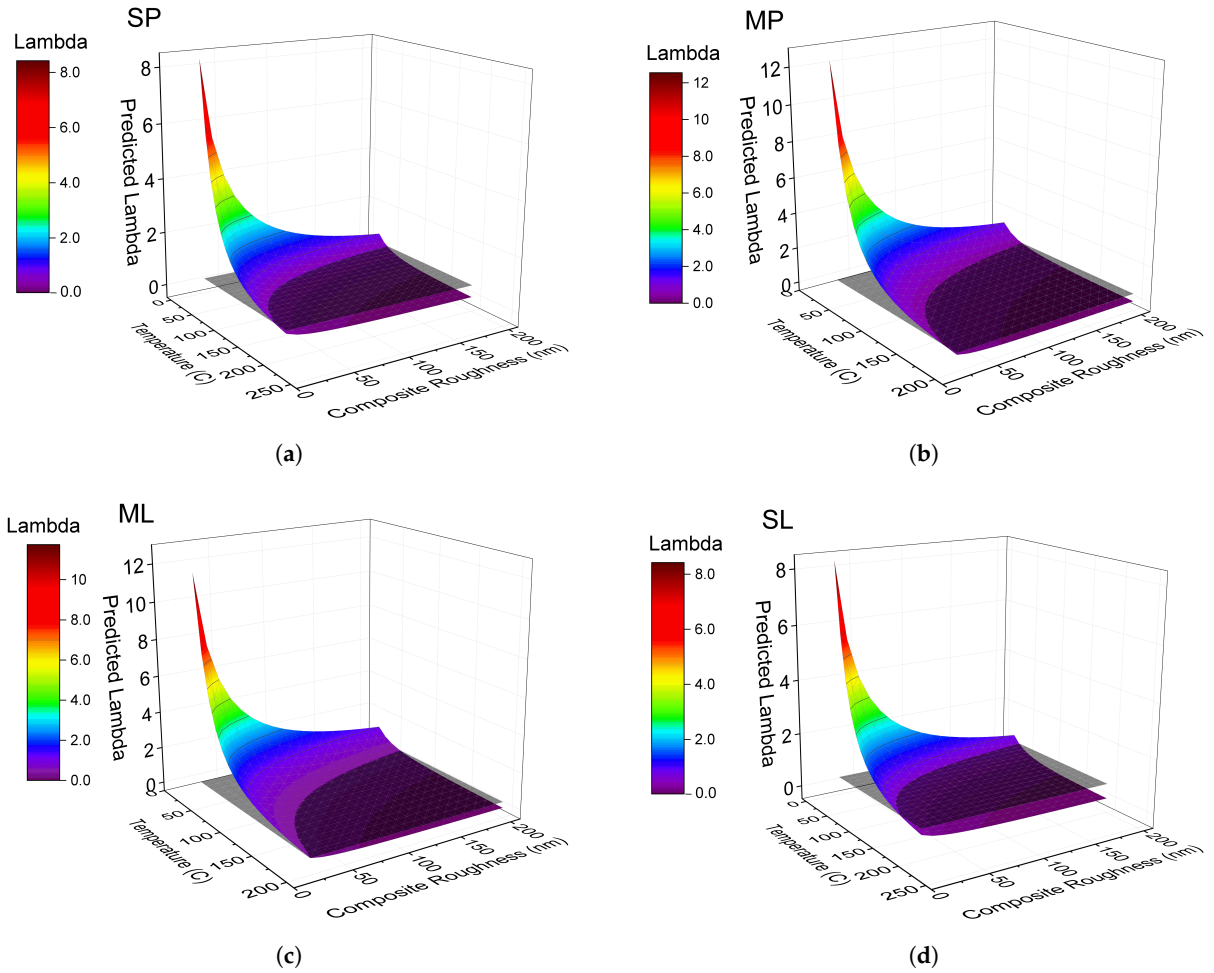

Figure 7. Contour plots with predicted λ ratios for each of the four commercially available EM greases: (**a**) SP, (**b**) MP, (**c**) ML, and (**d**) SL. The transition between full film and mixed lubrication (λ_t) is shown as a horizontal plane.

4.3. Grease Evaluation

The four greases evaluated in this study exhibited varying levels of performance at different surface roughness and temperature conditions. These observations are summarized briefly here.

As observed in Figure 2a, MP had the lowest wear rate on smooth surfaces, while ML had the lowest wear on rough surfaces. ML was also found to exhibit the least dependence of wear rate on surface roughness. On average, greases with mineral base oil had lower wear rate and roughness dependence than the synthetic base greases. In high temperature tests (150 °C), the lowest wear rate was found for the SL grease. In addition, the wear rate of the synthetic greases did not change with temperature at high temperatures, while an increase in wear rate with temperature was observed for the mineral greases. In the 4-ball tests, ML had the lowest wear across all the various bearing configurations. For the SS^3 and NS^3 configurations, average wear increased as ML < MP < SP < SL. Larger wear rates increase material debris, which can have implications, such as artificial surface roughness, reduced lubricating capabilities, and abrasion/erosion, so low wear is extremely important.

In terms of friction, on most surfaces, friction was lowest for the SL grease. For rougher surfaces, the lithium greases generally had lower friction than the polyurea greases. On very smooth surfaces, the synthetics had lower friction than the mineral based greases. In terms of temperature, at 40 °C, the lowest friction was exhibited by the SP grease whereas,

at 100 °C, the SL grease had the lowest friction. At both 40 and 100 °C, the friction was lower for synthetic greases than their mineral counterparts. The friction data was also used to determine transitions between the full film and mixed lubrication regime. This analysis showed that under these testing parameters, ML had the lowest λ_t, indicating that the interface would remain in the full film regime the longest with increasing temperature or roughness. However, ML also had higher friction in this transition region indicating that the lubricant maintained a thicker lubrication film at a cost of higher viscous friction. In contrast, SL had a larger λ_t ratio but considerably lower friction than the rest of the tested greases in this range.

While the comparisons between greases in terms of individual performance metrics are valuable, they need to be combined to determine which grease is best for a given application. Therefore, it is necessary to develop a grease evaluation and comparison method to assess these commercially available greases. Performance metrics included are low temperature (40 °C) friction, low surface roughness (10–60 nm Ra) friction and wear, high surface roughness (120–200 nm Ra) friction and wear, high temperature (100–150 °C) friction and wear, wear dependence on surface roughness, and NS^3 (best represents EM hybrid bearings) wear from the 4-ball tests. The ranking system was developed with EM bearing applications in mind, so high temperature friction and wear were given twice the weight of the other metrics. The greases were ranked 1 through 4 (or 8 for high temperature parameters), where 4 (or 8) was best. The results are shown as radar plots in Figure 8.

The individual rankings for each grease were summed to give an overall score, shown next to the radar plots in Figure 8. Based on the overall score, for the testing parameters used here, the two lithium greases outperformed the two polyurea greases (SL = 34 > ML = 31 > SP = 25 > MP = 22). The overall score can also be separated into a friction rating and a wear rating, both of which are reported next to the radar plots in Figure 8. In terms of friction performance, the results indicate that the synthetic greases had better overall friction performance than the mineral based greases (SL = 19 > SP = 14 > ML = 10 > MP = 7). Consistent with the overall rating, SL exhibited the best friction performance, particularly at high temperatures. However, different trends are observed for wear, and the overall wear scores indicate that mineral greases outperformed their synthetic counterparts (ML = 21 > SL = 15, MP = 15 > SP = 11). The ML exhibited the best wear performance and, particularly, the least dependence of wear on surface roughness. MP and SL were tied for the second-best, but the good rating of SL was largely due to its low wear at high temperature whereas MP outperformed SL in all other wear metrics, particularly wear at low surface roughness.

Generally, the overall ratings, along with the radar charts themselves, serve as guidelines with which a designer can evaluate each grease based on metrics important for the application being considered. However, it should be noted that long duration and high speed bearing/grease life tests would be useful as another metric to include in this type of analysis for grease evaluation for EM applications.

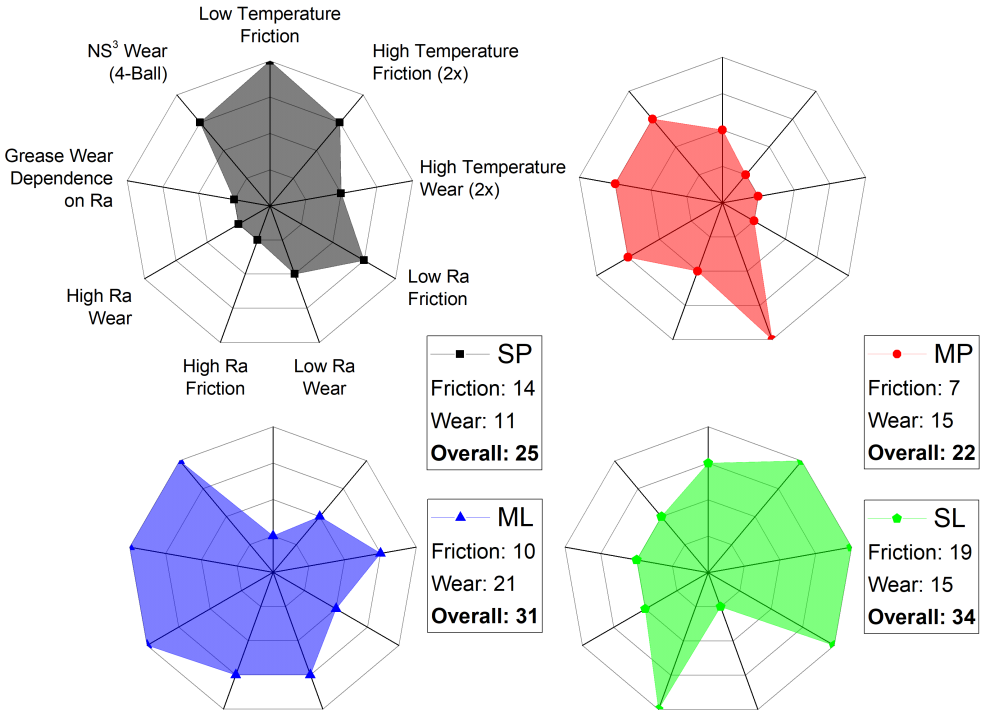

Figure 8. Grease ranking system based on a 1 to 4 scale (or 1 to 8 for high temperature parameters). A ranking of 4 (8) corresponds to best and 1 to worst. Low temperature is 40 °C, high temperature is 100–150 °C, low Ra is from 10–60 nm Ra, and high Ra from 120–200 nm Ra.

5. Conclusions

The tribological behavior of commercially available EM greases on hybrid bearing materials was characterized and evaluated. Results showed that EM grease products have notable differences in performance across different roughness and temperature conditions. These variations in performance have important implications for lubrication and design limitations. In general, greases whose performance is least affected by changing operating conditions will be more likely to meet the tribological needs of EMs.

Surface roughness has a significant impact on tribological properties. Rougher surfaces generally correspond to more friction and wear since they tend to have smaller local film thickness and higher pressure at asperity peaks [34,42,43], which result in high shear rates and stresses [12,42,43]. In contrast, surfaces with low roughness increase grease life and are less demanding in terms of lubrication ability since interacting smooth surfaces are more easily separated by lubricating films [8]. Yet, extremely smooth surfaces risk sudden seizure and asperities on rough surfaces may be useful for retaining lubricant [2]. Therefore, surface roughness plays a key role in determining the performance of grease lubricated systems.

Another important parameter for grease tribology is temperature, particularly for high-speed bearings. EM grease is known to be susceptible to thermo-oxidation degradation during high temperature bearing operation [9], which can lead to grease lubrication failure and, consequently, bearing failure [4,9–11]. Thus, grease formulations that do not compromise lubrication capabilities at high temperatures and resist thermal-oxidation are likely to be better for lubricating EM bearings. Temperature also influences film thickness through its effect on viscosity and the pressure-viscosity coefficient. Low temperature environments may be beneficial to achieving thicker lubricating grease films and reduce wear but will increase viscous friction. Further, excessively thick and viscous grease films may cause contact starvation from poor grease bleed and lack of reflow [16], which also leads to an increase in friction [22]. On the other hand, an increase in temperature can reduce

viscous friction and activate grease bleed, but, under high temperatures, film thickness can decrease [16,22,44] to levels that may promote harsher operating conditions detrimental to grease and bearing life. Consequently, EM greases will need to be optimized for high operating temperatures and formulated to have minimal temperature dependence.

Both temperature and surface roughness affect the lubrication regime, as quantified by the λ ratio. Ideal λ ratios during operation will be small enough to achieve low friction but not so small that there is a transition into mixed or boundary lubrication. Ideal λ ratios can also have a positive effect on bearing contact fatigue, prolong component life, and improve energy efficiency. Therefore, maintaining a consistent λ ratio across temperature and roughness conditions is a key factor in component design and grease selection.

EM grease formulations also need to be optimized for hybrid bearing materials, assuming the continued use of hybrid bearings to combat stray current. Umbrella grease type products might not capture all lubrication requirements [34] and, consequently, may jeopardize performance and system life. Further, non-traditional bearing material and material configurations can exhibit wear mechanisms distinct from those observed in traditional steel bearings. The 4-ball test results reported here indicate the ideal hybrid bearing configuration is ceramic rolling elements on steel races (NS^3). The inverse bearing configuration, steel rolling elements on ceramic races (SN^3), generated significantly larger and abnormal wear. Additionally, the NS^3 configuration was found to have better wear performance than traditional SS^3 bearings, which has positive implications for hybrid bearings and grease life.

The results of a comprehensive set of friction and wear tests, using 4-ball tests and ball-on-disk measurements across a range of roughness and temperature conditions, showed that SL had the best overall performance under the conditions tested here (Figure 8). SL provided low wear at 40 nm Ra or less and consistently maintained low friction throughout both the full film and mixed lubrication regimes. When results were analyzed in terms of friction and wear separately, it was found that synthetic greases had the best friction behavior, while mineral greases had the best wear performance, with ML being best overall in terms of wear. However, ultimately grease selection will depend on the application. In the process of comparing four greases, this study also developed an approach for the λ ratio and the transition between lubrication regimes (Figure 7) that may be useful as a design tool more generally.

Going forward, the tribological performance of potential hybrid bearing materials combined with grease formulations for EMs need to be fully explored under conditions that resemble the environments of the target application. This is particularly important because tribology will play an important role enabling the electrification of the transportation industry, and, through tribological research, EM bearing lubrication can be optimized for EVs as it has been for ICEVs. In this context, the study reported here is a baseline and a template for further grease research in EM environments. Further, the present study demonstrates that market-available EM grease products can vary significantly in performance, providing insight into the effects of operating conditions and design criteria on grease behavior.

Author Contributions: Conceptualization, A.M. and D.S.G.; methodology, A.M. and D.S.G.; experiments, S.L. and D.S.G.; data curation, A.M. and D.S.G.; writing—original draft preparation, A.M. and D.S.G.; writing—review and editing, A.M., S.L. and D.S.G. All authors have read and agreed to the published version of the manuscript.

Funding: This research was supported by the National Lubricating Grease Institute (NLGI).

Acknowledgments: We appreciate the valuable input from our NLGI liaison throughout the project. We also acknowledge the UC Merced Instructional Lab Support Team and Instrumentation Foundry. Lastly, some of the 4-ball tests were performed by undergraduate students in the research group, Colin Cox, Alex McCollum, Jose Morales, and Eddie Santiago.

Conflicts of Interest: The authors declare no conflict of interest.

References

1. Nieuwenhuis, P.; Cipcigan, L.; Sonder, H.B. The Electric Vehicle Revolution. In *Future Energy*; Elsevier: Amsterdam, The Netherlands, 2020; pp. 227–243.
2. Stachowiak, G.; Batchelor, A. *Engineering Tribology*; Butterworth-Heinemann: Oxford, UK, 2013.
3. Farfan-Cabrera, L.I. Tribology of electric vehicles: A review of critical components, current state and future improvement trends. *Tribol. Int.* **2019**, *138*, 473–486. [CrossRef]
4. He, F.; Xie, G.; Luo, J. Electrical bearing failures in electric vehicles. *Friction* **2020**, *8*, 4–28. [CrossRef]
5. Lukaszczyk, M. Improving efficiency in electric motors. *World Pumps* **2014**, *2014*, 34–41. [CrossRef]
6. de Santiago, J.; Bernhoff, H.; Ekergård, B.; Eriksson, S.; Ferhatovic, S.; Waters, R.; Leijon, M. Electrical Motor Drivelines in Commercial All-Electric Vehicles: A Review. *IEEE Trans. Veh. Technol.* **2012**, *61*, 475–484. [CrossRef]
7. Walther, H.C.; Holub, R.A. Lubrication of electric motors as defined by IEEE standard 841-2009, shortcomings and potential improvement opportunities. In Proceedings of the 2014 IEEE Petroleum and Chemical Industry Technical Conference (PCIC), San Francisco, CA, USA, 8–10 September 2014; pp. 91–98.
8. Lugt, P.M. Modern advancements in lubricating grease technology. *Tribol. Int.* **2016**, *97*, 467–477. [CrossRef]
9. Yu, Z.; Yang, Z. Fatigue failure analysis of a grease-lubricated roller bearing from an electric motor. *J. Fail. Anal. Prev.* **2011**, *11*, 158–166. [CrossRef]
10. Fernandes, P. Contact fatigue in rolling-element bearings. *Eng. Fail. Anal.* **1997**, *4*, 155–160. [CrossRef]
11. Fernandes, P.; McDuling, C. Surface contact fatigue failures in gears. *Eng. Fail. Anal.* **1997**, *4*, 99–107. [CrossRef]
12. Kanazawa, Y.; Sayles, R.S.; Kadiric, A. Film formation and friction in grease lubricated rolling-sliding non-conformal contacts. *Tribol. Int.* **2017**, *109*, 505–518. [CrossRef]
13. Cann, P. Grease lubrication of rolling element bearings—Role of the grease thickener. *Lubr. Sci.* **2007**, *19*, 183–196. [CrossRef]
14. Cousseau, T.; Graça, B.; Campos, A.; Seabra, J. Grease aging effects on film formation under fully-flooded and starved lubrication. *Lubricants* **2015**, *3*, 197–221. [CrossRef]
15. Zapletal, T.; Sperka, P.; Krupka, I.; Hartl, M. On the Relation between Friction Increase and Grease Thickener Entraining on a Border of Mixed EHL Lubrication. *Lubricants* **2020**, *8*, 12. [CrossRef]
16. Cann, P. Starved grease lubrication of rolling contacts. *Tribol. Trans.* **1999**, *42*, 867–873. [CrossRef]
17. De Laurentis, N.; Kadiric, A.; Lugt, P.; Cann, P. The influence of bearing grease composition on friction in rolling/sliding concentrated contacts. *Tribol. Int.* **2016**, *94*, 624–632. [CrossRef]
18. Cen, H.; Lugt, P.M.; Morales-Espejel, G. On the film thickness of grease-lubricated contacts at low speeds. *Tribol. Trans.* **2014**, *57*, 668–678. [CrossRef]
19. Cen, H.; Lugt, P.M. Film thickness in a grease lubricated ball bearing. *Tribol. Int.* **2019**, *134*, 26–35. [CrossRef]
20. Cen, H.; Lugt, P.M.; Morales-Espejel, G. Film thickness of mechanically worked lubricating grease at very low speeds. *Tribol. Trans.* **2014**, *57*, 1066–1071. [CrossRef]
21. Morales-Espejel, G.; Lugt, P.M.; Pasaribu, H.; Cen, H. Film thickness in grease lubricated slow rotating rolling bearings. *Tribol. Int.* **2014**, *74*, 7–19. [CrossRef]
22. Gonçalves, D.E.; Campos, A.V.; Seabra, J.H. An experimental study on starved grease lubricated contacts. *Lubricants* **2018**, *6*, 82. [CrossRef]
23. Sebastian, T. Temperature effects on torque production and efficiency of PM motors using NdFeB magnets. *IEEE Trans. Ind. Appl.* **1995**, *31*, 353–357. [CrossRef]
24. Hamidizadeh, S.; Alatawneh, N.; Chromik, R.R.; Lowther, D.A. Comparison of different demagnetization models of permanent magnet in machines for electric vehicle application. *IEEE Trans. Magn.* **2016**, *52*, 1–4. [CrossRef]
25. Lugt, P.M. *Grease Lubrication in Rolling Bearings*; John Wiley & Sons: Hoboken, NJ, USA, 2012.
26. Oliver, J.; Guerrero, G.; Goldman, J. Ceramic bearings for electric motors. In Proceedings of the 2015 IEEE-IAS/PCA Cement Industry Conference (IAS/PCA CIC), Toronto, ON, Canada, 26–30 April 2015; pp. 1–11.
27. Gonda, A.; Capan, R.; Bechev, D.; Sauer, B. The Influence of Lubricant Conductivity on Bearing Currents in the Case of Rolling Bearing Greases. *Lubricants* **2019**, *7*, 108. [CrossRef]
28. Dante, R.C.; Kajdas, C. A review and a fundamental theory of silicon nitride tribochemistry. *Wear* **2012**, *288*, 27–38. [CrossRef]
29. Volante, M.; Fubini, B.; Giamello, E.; Bolis, V. Reactivity induced by grinding in silicon nitride. *J. Mater. Sci. Lett.* **1989**, *8*, 1076–1078. [CrossRef]
30. Zaretsky, E.V.; Vlcek, B.L.; Hendricks, R.C. Effect of silicon nitride balls and rollers on rolling bearing life. *Tribol. Trans.* **2005**, *48*, 425–435. [CrossRef]
31. Johnson, D.W. *The Tribology and Chemistry of Phosphorus Containing Lubricant Additives*; IntechOpen: London, UK, 2016.
32. Bertrand, P. Reactions of tricresyl phosphate with bearingmaterials. *Tribol. Lett.* **1997**, *3*, 367–377. [CrossRef]
33. Guan, B.; Pochopien, B.A.; Wright, D.S. The chemistry, mechanism and function of tricresyl phosphate (TCP) as an anti-wear lubricant additive. *Lubr. Sci.* **2016**, *28*, 257–265. [CrossRef]
34. Gonçalves, D.; Vieira, A.; Carneiro, A.; Campos, A.V.; Seabra, J.H. Film thickness and friction relationship in grease lubricated rough contacts. *Lubricants* **2017**, *5*, 34. [CrossRef]
35. Chang, H.; Lan, C.; Chen, C.; Kao, M.; Guo, J. Anti-wear and friction properties of nanoparticles as additives in the lithium grease. *Int. J. Precis. Eng. Man.* **2014**, *15*, 2059–2063. [CrossRef]

36. Qiang, H.; Anling, L.; Yangming, Z.; Liu, S.; Yachen, G. Experimental study of tribological properties of lithium-based grease with Cu nanoparticle additive. *Tribol.-Mater. Surf. Interfaces* **2017**, *11*, 75–82. [CrossRef]
37. Qiang, H.; Anling, L.; Yachen, G.; Songfeng, L.; LH, K. Effect of nanometer silicon dioxide on the frictional behavior of lubricating grease. *Nanomater. Nanotechnol.* **2017**, *7*, 1–9.
38. Gow, G. Lubricating grease. In *Chemistry and Technology of Lubricants*; Springer: Berlin/Heidelberg, Germany, 1992; pp. 255–268.
39. Strunks, G.; Toth, D.; Saba, C. Geometry of wear in the sliding four-ball wear test. *Tribol. Trans.* **1992**, *35*, 715–723. [CrossRef]
40. Walters, N.; Martini, A. Friction dependence on surface roughness for castor oil lubricated NiTi alloy sliding on steel. *Tribol. Trans.* **2018**, *61*, 1162–1166. [CrossRef]
41. Hansen, J.; Björling, M.; Larsson, R. Lubricant film formation in rough surface non-conformal conjunctions subjected to GPa pressures and high slide-to-roll ratios. *Sci. Rep.* **2020**, *10*, 22250. [CrossRef]
42. Guegan, J.; Kadiric, A.; Spikes, H. A study of the lubrication of EHL point contact in the presence of longitudinal roughness. *Tribol. Lett.* **2015**, *59*, 22. [CrossRef]
43. Guegan, J.; Kadiric, A.; Gabelli, A.; Spikes, H. The relationship between friction and film thickness in EHD point contacts in the presence of longitudinal roughness. *Tribol. Lett.* **2016**, *64*, 33. [CrossRef]
44. Cann, P. Starvation and reflow in a grease-lubricated elastohydrodynamic contact. *Tribol. Trans.* **1996**, *39*, 698–704. [CrossRef]